U.S. National Library of Medicine
National Center for Biotechnology Information

NLM Citation: Zhang H. Eu-chelate anti-fibrin antibody-conjugated perfluorocarbon nanoparticles. 2008 Jan 17 [Updated 2008 Feb 20]. In: Molecular Imaging and Contrast Agent Database (MICAD) [Internet]. Bethesda (MD): National Center for Biotechnology Information (US); 2004-2013.
Bookshelf URL: https://www.ncbi.nlm.nih.gov/books/

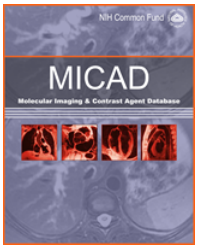

Eu-chelate anti-fibrin antibody-conjugated perfluorocarbon nanoparticles

EuPFC

Huiming Zhang, PhD[1]

Created: January 17, 2008; Updated: February 20, 2008.

Chemical name:	Eu-chelate anti-fibrin antibody-conjugated perfluorocarbon nanoparticles	
Abbreviated name:	EuPFC	
Synonym:		
Agent category:	Antibody, small molecule (nanoparticle)	
Target:	Fibrin	
Target category:	Antigen	
Method of detection:	Magnetic resonance imaging (MRI), Ultrasound	
Source of signal/contrast:	Europium, perfluorocarbon	
Activation:	No	
Studies:	• *In vitro*	No structure is available in PubChem.

Background

[PubMed]

Acute thrombus formation after atherosclerotic plaque rupture has been well recognized as the cause of unstable angina, myocardial infarction, transient ischemic attack, and stroke (1, 2). Platelets and fibrin are the major components of all thrombi involved in the development and progression of atherosclerotic disease (3). Magnetic resonance imaging (MRI) has shown promise in thrombus detection in both animals and humans (4), either with direct thrombus imaging based on the T_1-shortening properties of endogenous methemoglobin in venous thrombi (5) or by enhancement of the contrast between the myocardium and intracardiac tissues by conventional gadolinium (Gd) chelates (6). However, thrombosis is a dynamic process in which thrombus material of different ages forms a layered structure as a result of successive mural deposition (7). The MRI signal of a thrombus is complicated by the presence of platelets, fibrin, and red blood cells in the clots (7). Accurate thrombus age definition and detection of old and organized thrombi remain difficult. Because fibrin is abundant in all types of thrombi, including arterial, venous, acute, and chronic, contrast agents that target fibrin can be used to differentiate between layers of fibrin deposits in all types of thrombi and in superimposed thrombosis

Author Affiliation: 1 National Center for Biotechnology Information, NLM, NIH, Bethesda, MD; Email: micad@ncbi.nlm.nih.gov.

associated with plaque (3). Fibrin is formed after thrombin cleavage of fibrinopeptide A from fibrinogen Aα-chains, followed by polymerization and cross-linkage to form thick fibrin bundles and complex, branched-clot networks (8). The low concentration of fibrin present in plasma minimizes spurious background imaging signals (3).

Europium(III) (Eu^{3+}) is a lanthanide cation with six unpaired electrons in the f-shell. Many of the physical and chemical properties of Eu^{3+} are similar to those of its neighbor Gd(III) (Gd^{3+}), which has seven unpaired electrons. However, the spin interactions between Eu^{3+} and its directly bound water molecules are quite different from the spin interactions between Gd^{3+} and its directly bound water molecules. Both Gd^{3+} and Eu^{3+} exhibit a large effective magnetic momentum to generate a paramagnetic effect. The electron relaxation time of Eu^{3+} (10^{-12}–10^{-13} s) is between four and five orders of magnitude shorter than that of Gd^{3+} (10^{-8}–10^{-9}s) (9). The pseudocontact shift is quite large for Eu^{3+}, but it is zero for Gd^{3+} (9). As a result, Gd chelates are used as T_1-relaxation agents in MRI because of a strong enhancement effect in T_1 relaxation; Eu chelates are used as a chemical shift agent in nuclear magnetic resonance spectroscopy because they induce a substantial chemical shift effect. Eu^{3+} has a negligible effect on water proton T_1 relaxivity because of its short electron relaxation time (9, 10). Similar to Gd-1,4,7,10-tetraazcyclododecane-*N,N',N",N"'*-tetraacetate (Gd-DOTA), Eu-DOTA has one coordinated water molecule in exchange with bulk water. The water residual time (τ_m) can be prolonged to sub-millisecond scale by substitution of DOTA with various hydrophilic groups that drag the water exchange kinetics into slow exchange region ($\Delta\omega\tau_m >> 1$) (11). Here $\Delta\omega$ is the chemical shift difference between water molecules bound to the metal cation and bulk water, and its value is ~50 ppm for Eu^{3+} (12, 13). Radiofrequency prepulses applied at the appropriate frequency and power level can saturate Eu^{3+}-bound water molecules. The exchange between the bound water and the bulk water pool leads to reduced equilibrium magnetization for bulk water (11). This negative imaging contrast, called paramagnetic chemical exchange saturation transfer (PARACEST) contrast (11), is "switched on" by simply changing the pulse sequence parameters, a unique feature of MRI. Simultaneously, the prepulse also generates magnetization transfer (MT) effect between the exchangeable protons in tissues (-NH, -OH, *etc.*) with bulk water. The MT effect produces a magnetization profile (Z-spectrum) of bulk water that is symmetrical about the chemical shift of bulk water (14, 15). Thus, a net change that originated from the PARACEST effect can be obtained by subtraction of images collected at ± frequency offset of the presaturation pulses. In general, signal change in bulk water is 37% for ~100 μM PARACEST agent and 5% for ~10 μM PARACEST agent (11). A major advantage of PARACEST contrast is easy detection of the targeted agent without the need to collect images before and after contrast administration (16).

Eu chelate anti-fibrin antibody–conjugated perfluorocarbon (PFC) nanoparticles (EuPFC) are a MRI PARACEST agent used to image fibrin (16). EuPFC consists of three components (i.e., biotinylated phospholipids, Eu chelate–conjugated phospholipid, and monolayer lipid-encapsulated PFC nanoparticles). The biotinylated phospholipids provide convenience for site-directed targeting. The PFC nanoparticle has a liquid core that is ~200–250 nm in diameter and is emulsified through a microfluidization technique at 20,000 psi. Historically, PFC emulsions have been used as blood substitutes as a result of its high O_2-loading capacity and excellent biological inertness (17). Recently, PFC emulsions have been adopted for use as principal components in ultrasound contrast agents because of their low acoustic impedance relative to that of soft tissues (18). Unlike microbubble-based formulations, the nanoparticles produce a negligible signal in circulation until they are bound and concentrated at a specific target. The prolonged systematic half-life of EuPFC (β-elimination time was ~1 h) provides adequate time for the nanoparticles to saturate targeted binding sites (19). The large surface of a PFC can be modified to carry a substantial amount of targeting ligands (antibodies, peptides, biotins) and imaging payloads used in MRI, nuclear imaging, and computed tomography (20). For instance, a PFC nanoparticle can support up to 50,000–100,000 Gd chelates, which allows robust detection of target molecules in the pM range by MRI (20). This also creates a bifunctional ultrasonic contrast agent that can be used in combination with other imaging modalities.

Synthesis

[PubMed]

Winter et al. briefly described the synthesis of EuPFC (16). Commercially available 1-(2-methyloxy-5-amine-benzyl)-tetra-glycine ethyl-1,4,7,10 tetraazacyclododecane-1,4,7,10-tetraacetate was coupled to a phosphatidylethanolamine through a thiourea linkage to the amine on the phenyl ring. Eu^{3+} was added at equimolar concentrations to form the PARACEST agent, abbreviated as Eu^{3+}-methoxyl-benzyl-DOTA. PFC nanoparticles were obtained by emulsion of 15% (v/v) perfluorooctyl bromide (PFOB, $C_8F_{17}Br$), 1% (w/v) surfactant co-mixture, 2.5% (w/v) glycerin, and water in a microfluidizer for 4 min at 20,000 psi. The co-mixture was a liposome suspension made from a chloroform solution of 64 mol% lecithin, 35 mol% cholesterol, and 1 mol% N-((6-(biotinoyl)amino)hexanoyl)-dipalmitoyl-L-alpha-phosphatidylethanolamine. The obtained PFC nanoparticles were functionalized with a surfactant comprising phosphatidylcholine, biotinylated dipalmitoylphosphatidylethanolamine, and Eu^{3+}-methoxyl-benzyl-DOTA at a molar ratio of 59:1:40. The size of the nanoparticles was measured with electrophoretic light-scattering/laser Doppler velocimetry. The diameter was found to be 294 nm with a distribution of 0.215. The Eu^{3+} content was determined by standard comparator instrumental neutron activation analysis. The concentration of Eu^{3+} in the EuPFC emulsion was 2.1 mM.

In Vitro Studies: Testing in Cells and Tissues

[PubMed]

Winter et al. conducted a series of imaging and spectroscopy studies on a 4.7-T imager (16). First, proton spectra of bulk water were collected for both EuPFC and control PFC nanopartciles using a 2-s presaturation pulse at a power level of 28 dB. The magnetization of bulk water was plotted as a function of frequency offset that ranged from 100 ppm to +100 ppm (relative to the bulk water frequency of 0 ppm. Compared to the control nanoparticles, EuPFC exhibited a marked saturation contrast effect at a presaturation frequency of +52 ppm. Second, the enhancement effect of EuPFC was examined in a two-compartment phantom in which EuPFC and control nanoparticles were located in separate chambers. Images were collected with the use of 2.5-s presaturation pulses at a power level of 38 dB with frequency offset of ±52 ppm relative to the bulk water peak. Subtraction of the images collected with saturation at +52 ppm from the images collected at -52 ppm demonstrated an 11.7% image enhancement in the compartment with EuPFC compared to the control nanoparticles. The enhancement effect of EuPFC was then examined in cylindrical plasma clots suspended in sterile saline. The acellular clots were formed in a plastic mold (5 mm in diameter) by combining fresh dog plasma with 5 U of thrombin and $CaCl_2$. Subsequently, the clots were incubated with 150 μg biotinylated anti-fibrin antibodies (1H10) overnight followed by 50 μg avidin for 1 h, then 250 μl of EuPFC for 1 h. The images were acquired with parameters identical to those used for the two-compartment phantom. After the subtraction of the images collected with saturation at +52 ppm from the images collected at -52 ppm, the surface of the clot treated with fibrin-targeted EuPFC appeared to have ~10% enhancement in signal intensity and could be clearly distinguished from the rest.

Animal Studies

Rodents

[PubMed]

No publication is currently available.

Other Non-Primate Mammals

[PubMed]

No publication is currently available.

Non-Human Primates

[PubMed]

No publication is currently available.

Human Studies

[PubMed]

No publication is currently available.

NIH Support

CO 07121, HL 42950, HL 59865, EB 01704

References

1. Libby P. Current concepts of the pathogenesis of the acute coronary syndromes. Circulation. 2001;104(3):365–72. PubMed PMID: 11457759.
2. Briley-Saebo K.C., Mulder W.J., Mani V., Hyafil F., Amirbekian V., Aguinaldo J.G., Fisher E.A., Fayad Z.A. Magnetic resonance imaging of vulnerable atherosclerotic plaques: current imaging strategies and molecular imaging probes. J Magn Reson Imaging. 2007;26(3):460–79. PubMed PMID: 17729343.
3. Sirol M., Aguinaldo J.G., Graham P.B., Weisskoff R., Lauffer R., Mizsei G., Chereshnev I., Fallon J.T., Reis E., Fuster V., Toussaint J.F., Fayad Z.A. Fibrin-targeted contrast agent for improvement of in vivo acute thrombus detection with magnetic resonance imaging. Atherosclerosis. 2005;182(1):79–85. PubMed PMID: 16115477.
4. Yuan C., Kerwin W.S., Yarnykh V.L., Cai J., Saam T., Chu B., Takaya N., Ferguson M.S., Underhill H., Xu D., Liu F., Hatsukami T.S. MRI of atherosclerosis in clinical trials. NMR Biomed. 2006;19(6):636–54. PubMed PMID: 16986119.
5. Viereck J., Ruberg F.L., Qiao Y., Perez A.S., Detwiller K., Johnstone M., Hamilton J.A. MRI of atherothrombosis associated with plaque rupture. Arterioscler Thromb Vasc Biol. 2005;25(1):240–5. PubMed PMID: 15528478.
6. Ala-Korpela M., Sipola P., Kaski K. Characterization and molecular detection of atherothrombosis by magnetic resonance--potential tools for individual risk assessment and diagnostics. Ann Med. 2006;38(5):322–36. PubMed PMID: 16938802.
7. Botnar R.M., Perez A.S., Witte S., Wiethoff A.J., Laredo J., Hamilton J., Quist W., Parsons E.C. Jr, Vaidya A., Kolodziej A., Barrett J.A., Graham P.B., Weisskoff R.M., Manning W.J., Johnstone M.T. In vivo molecular imaging of acute and subacute thrombosis using a fibrin-binding magnetic resonance imaging contrast agent. Circulation. 2004;109(16):2023–9. PubMed PMID: 15066940.
8. Mosesson M.W. Fibrinogen and fibrin structure and functions. J Thromb Haemost. 2005;3(8):1894–904. PubMed PMID: 16102057.
9. Peters J.A., Huskens J., Raber D.J. Lanthanide induced shifts and relaxation rate enhancements. Prog. NMR Spectrosc. 1996;28:283.
10. Geraldes C.F. Lanthanide shift reagents. Methods Enzymol. 1993;227:43–78. PubMed PMID: 8255231.

11. Zhang S., Merritt M., Woessner D.E., Lenkinski R.E., Sherry A.D. PARACEST agents: modulating MRI contrast via water proton exchange. Acc Chem Res. 2003;36(10):783–90. PubMed PMID: 14567712.
12. Zhang S., Wu K., Biewer M.C., Sherry A.D. 1H and (17)O NMR detection of a lanthanide-bound water molecule at ambient temperatures in pure water as solvent. Inorg Chem. 2001;40(17):4284–90. PubMed PMID: 11487334.
13. Zhang S., Winter P., Wu K., Sherry A.D. A novel europium(III)-based MRI contrast agent. J Am Chem Soc. 2001;123(7):1517–8. PubMed PMID: 11456734.
14. Wolff S.D., Balaban R.S. Magnetization transfer contrast (MTC) and tissue water proton relaxation in vivo. Magn Reson Med. 1989;10(1):135–44. PubMed PMID: 2547135.
15. Ward K.M., Aletras A.H., Balaban R.S. A new class of contrast agents for MRI based on proton chemical exchange dependent saturation transfer (CEST). J Magn Reson. 2000;143(1):79–87. PubMed PMID: 10698648.
16. Winter P.M., Cai K., Chen J., Adair C.R., Kiefer G.E., Athey P.S., Gaffney P.J., Buff C.E., Robertson J.D., Caruthers S.D., Wickline S.A., Lanza G.M. Targeted PARACEST nanoparticle contrast agent for the detection of fibrin. Magn Reson Med. 2006;56(6):1384–8. PubMed PMID: 17089356.
17. Spahn D.R. Blood substitutes. Artificial oxygen carriers: perfluorocarbon emulsions. Crit Care. 1999;3(5):R93–7. PubMed PMID: 11094488.
18. Lanza G.M., Wallace K.D., Scott M.J., Cacheris W.P., Abendschein D.R., Christy D.H., Sharkey A.M., Miller J.G., Gaffney P.J., Wickline S.A. A novel site-targeted ultrasonic contrast agent with broad biomedical application. Circulation. 1996;94(12):3334–40. PubMed PMID: 8989148.
19. Marsh J.N., Hall C.S., Scott M.J., Fuhrhop R.W., Gaffney P.J., Wickline S.A., Lanza G.M. Improvements in the ultrasonic contrast of targeted perfluorocarbon nanoparticles using an acoustic transmission line model. IEEE Trans Ultrason Ferroelectr Freq Control. 2002;49(1):29–38. PubMed PMID: 11833889.
20. Winter P.M., Cai K., Caruthers S.D., Wickline S.A., Lanza G.M. Emerging nanomedicine opportunities with perfluorocarbon nanoparticles. Expert Rev Med Devices. 2007;4(2):137–45. PubMed PMID: 17359221.